A Novel Mechanism of Modulation of 5-HT$_3$A Receptors by Hydrocortisone

Jeremías Corradi, Natalia Andersen, and Cecilia Bouzat*
Instituto de Investigaciones Bioquímicas de Bahía Blanca. Universidad Nacional del Sur-CONICET, Bahía Blanca, Argentina

ABSTRACT Modulation of Cys-loop receptors by steroids is of physiological and therapeutical relevance. Nonetheless, its molecular mechanism has not been elucidated for serotonin (5-HT) type 3 receptors. We deciphered the mechanism of action of hydrocortisone (HC) at 5-HT type 3A receptors. Single-channel currents from the high-conductance form (~4.7 pA, −70 mV) appear as a series of long opening events forming bursts, which group into long clusters. Although they are very infrequent, subconductance events (~2.4 pA) are detected within clusters. HC produces a significant concentration-dependent reduction in open and burst durations, demonstrating open-channel block. In addition, it increases the appearance of subconductance levels in a concentration- and slightly voltage-dependent manner. The amplitude of the subconductance level does not change with HC concentration and its open duration is briefer than that of full amplitude events, indicating lower open-channel stability. Dual effects are distinguished from macroscopic responses: HC reduces amplitude by acting from either open or closed states, and it increases decay rates from the open state. Thus, HC acts as a negative modulator of 5-HT type 3A receptors by different mechanisms: It acts as an open-channel blocker and it favors opening to a preexisting subconductance level. The latter constitutes a novel, to our knowledge, mechanism of channel modulation, which might be applicable to other steroids and channels.

INTRODUCTION

Serotonin type 3 receptors (5-HT$_3$Rs) are members of the Cys-loop receptor family of neurotransmitter-gated ion channels, which also includes GABA$_A$, glycine, and nicotinic acetylcholine (ACh) receptors (1). 5-HT$_3$Rs are located predominantly in central nervous system regions that are involved in the integration of the vomiting reflex, pain processing, and anxiety control. The preferential localization on nerve endings is consistent with a physiological role of 5-HT$_3$Rs in the control of neurotransmitter release (2). They are implicated in several human disorders, such as anxiety, depression, and vomiting, and are important drug targets for nausea and emesis during pregnancy or provoked by drugs used in cancer therapy (3).

Steroids modulate function of Cys-loop receptors (4–9). They can act as negative (6,8–10) or positive allosteric modulators (11,12), depending on both the steroid and receptor types. Single-channel recordings have allowed researchers to describe the mechanisms of action of several steroids acting on AChRs and GABA$_A$ receptors (6,12). For 5-HT$_3$Rs, these studies have been restricted to the macroscopic level, and have shown that several steroids, such as 17-β-estradiol (9,10), progesterone, estradiol, mestranol, testosterone, and allopregnanolone (9), and dexamethasone and methylprednisolone (8), inhibit macroscopic serotonin type 3A (5-HT$_3$A) currents by acting as noncompetitive inhibitors. No detailed information about molecular effects of steroids at 5-HT$_3$ARs is available, because the low conductance of this receptor does not allow the detection of single-channel events.

The low single-channel conductance of the 5-HT$_3$AR has been shown to be due to the unique presence of three arginine residues (R432, R436, and R440) at the M3-M4 region (13–17). Elegant studies have shown that the replacement of these arginine residues by those found at equivalent positions in the 5-HT3B subunit (glutamine, aspartic acid, and alanine (QDA)) increases the single-channel conductance by ~40-fold, thus resulting in the high-conductance or QDA form of 5-HT$_3$AR (13,14,17).

We recently described the mechanism of activation and desensitization of the high-conductance form of the mouse 5-HT$_3$AR (18). We here took advantage of this high-conductance form to analyze the effects of hydrocortisone at the single-channel level. By detecting conformational states that cannot be resolved at the macroscopic level, we demonstrate that this steroid acts as a negative modulator of 5-HT$_3$ARs by two different mechanisms: it acts as an open-channel blocker and it simultaneously favors opening to a subconductance level.

METHODS

Expression of high-conductance 5-HT$_3$A receptors

The high-conductance form of mouse serotonin type 3A receptor (5-HT$_3$A) was obtained by mutating three arginine residues to QDA (13–19). Point mutations were introduced using the QuikChange kit (Stratagene, La Jolla, CA) and were confirmed by sequencing. BOSC 23 cells were transfected with 5-HT$_3$A cDNA and a plasmid encoding green fluorescent protein to allow identification of transfected cells.

Patch-clamp recordings

Single-channel currents were recorded in the cell-attached configuration at 20°C. The bath and pipette solutions contained 142 mM KCl, 5.4 mM NaCl, 0.2 mM $CaCl_2$, and 10 mM HEPES (pH 7.4) (18,19). 5-HT and

Submitted June 25, 2010, and accepted for publication October 27, 2010.

*Correspondence: inbouzat@criba.edu.ar

Editor: David S. Weiss.

0006-3495/11/01/0042/10 $2.00

doi: 10.1016/j.bpj.2010.10.046

hydrocortisone (HC) were added to the pipette solution. Patch pipettes were pulled from 7052 capillary tubes (Garner Glass, Claremont, CA) and coated with Sylgard (Dow Corning, Midland, MI). Single-channel currents were recorded and low-pass filtered to 10 kHz using an Axopatch 200 B patch-clamp amplifier (Molecular Devices, Union City, CA), digitized at 5-μs intervals, and detected by the half-amplitude threshold criterion using the TAC 4.0.10 program (Bruxton, Seattle, WA) (19). Under the present conditions, the inward conductance of the QDA 5-HT$_3$A mouse receptor, determined from single-channel amplitudes at different potentials, is ~67 pS (18).

The analysis of single-channel recordings was performed by tracking events without any amplitude restriction. This procedure involved the detection of all events in the whole recording in only one step and was the one used to determine the amplitude classes and their relative areas. Amplitude histograms were then constructed after selecting events with open duration >90 μs to assure that all events were fully resolved. However, no changes were observed in the mean amplitude of each class if the dead time was set between 30 and 500 μs. Open- and closed-time histograms were plotted using a logarithmic abscissa and a square-root ordinate, and fitted to the sum of exponential functions by maximum likelihood using the program TACFit 4.0.10 (Bruxton) with the dead time set at 30 μs. To determine the mean duration of each amplitude class, open-time histograms were constructed for a given amplitude class by selecting only openings with amplitudes within $\pm$1 pA of the mean of the amplitude class. Another analysis method was used to increase the number of subconductance opening events. This was performed by setting the detection bar to a fixed amplitude (2.4 pA) and then detecting channel events by the half-amplitude threshold criterion (20). The duration histogram was then constructed from the accepted events. No significant difference in the mean open duration was observed between the two types of analysis (20).

Bursts and clusters of channel openings were identified as a series of closely separated openings (more than five) preceded and followed by closings longer than a critical duration. For the control condition, the critical time was taken as the point of intersection of the second and third components in the closed-time histogram for bursts (τ_c^b), and of the third closed component and the succeeding one for clusters (τ_c^c) (18). In the presence of HC, τ_c^c was determined to be between the fourth and fifth closed components. For different recordings, τ_c^c values were 10 $\pm$ 3 ms for control, 18 $\pm$ 5 ms for 100 μM HC:, 40 $\pm$ 10 ms for 200 μM HC, and 50 $\pm$ 10 ms for 400 μM HC.

Open probability within clusters (P_{open}) was determined by calculating the mean fraction of time that the channel is open within a cluster (18,19).

All-point amplitude histograms were constructed with data obtained from clusters. Clusters were first identified by visual inspection and then selected using the TAC program. All-point histograms were then constructed with data from 10–20 selected clusters of each recording using TAC.

Macroscopic currents were recorded in the outside-out patch configuration. The pipette solution contained 134 mM KCl, 5 mM EGTA, 1 mM $MgCl_2$, and 10 mM HEPES (pH 7.3). The extracellular solution (ECS) contained 150 mM NaCl, 0.5 mM $CaCl_2$, and 10 mM HEPES (pH 7.4). We applied a 1.5-s pulse of ECS containing 100 μM 5-HT. The solution exchange time was estimated by the open pipette and varied between 0.1 and 1 ms. Macroscopic currents were filtered at 5 kHz, digitized at 20 kHz, and analyzed using the IgorPro software (WaveMetrics, Lake Oswego, OR). Each current represents the average from three to five individual traces obtained from the same seal that were aligned with each other at the point where they reached 50% of maximum. Currents were fitted by a double-exponential function:

$$I(t) = I_1(\exp(-t/\tau_1)) + I_2(\exp(-t/\tau_2)) + I_\infty, \quad (1)$$

where I_1 and I_2 are peak current values, and I_∞ is the steady-state current, respectively, and τ_1 and τ_2 are the decay time constants.

We recorded responses according to the different protocols for HC application: the +/− protocol, where the patch was exposed for 2 min to a bath solution containing the steroid before application of agonist; the −/+ protocol, consisting of exposure to a pulse of the agonist solution containing the steroid without preincubation; and the +/+ protocol, consisting of 2 min exposure to bath solution containing a specified concentration of steroid followed by a pulse of agonist solution also containing the steroid. All currents were analyzed with reference to those recorded in the same patch in the absence of HC (the −/− protocol). The stability of the patch and the absence of rundown were determined by verifying that the peak current remained constant after at least five pulses of agonist under each protocol. Patches showing rundown (>10–15% reduction of the peak current) were discarded.

Simulations of single-channel and macroscopic currents were performed using QuB software (QuB suite, www.qub.buffalo.edu, State University of New York, Buffalo, NY). For the simulations, we used the kinetic model that describes transitions within clusters and the estimated rate constants (18).

Statistical comparisons were performed with Student's *t*-test.

Docking of hydrocortisone in 5-HT$_3$A models

A homology model of two adjacent 5-HT3A subunits was created based on the structure of the *Torpedo* AChR (Protein Data Bank code 2BG9, A-E). The amino acid sequences were aligned using ClustalW and modeling was performed using MODELER 9v8 (21). Ten models were generated, of which the one with the lowest energy and the smallest percentage of amino acids in the disallowed region of the Ramachandran plot (calculated using PROCHECK) was selected for docking studies. The protonated form of HC was docked into the whole model or into the selected transmembrane region using AUTODOCK 4.2 (22). One hundred genetic algorithm runs were performed for each docking study.

RESULTS

Single-channel currents of 5-HT$_3$A receptors in the presence of hydrocortisone

In the presence of 5-HT (>0.1 μM), single-channel currents of ~4.7 pA at −70 mV membrane potential are readily detected in cell-attached patches from cells expressing the high-conductance form of mouse 5-HT$_3$A receptor (18,19) (Fig. 1). As reported previously (18), a minor population (<6%) of low-amplitude openings from the same receptor is also detected (~2.4 pA at −70 mV).

At 1 μM 5-HT, 5-HT$_3$A channel activity appears mainly as openings in quick succession forming bursts, which in turn coalesce into long clusters (18) (Fig. 1). A cluster results from the activity of a single receptor, which recovers from long-lived desensitization and begins a series of transitions through open and closed states. At the end of the cluster, the receptor reenters the desensitized state. Isolated brief openings or brief bursts are also detected along the recording (18) (Fig. 1 *b*).

Open-time histograms for the entire recording show three components, whose mean durations are ~115 μs, 2.5 ms, and 110 ms (18) (Fig.1 and Table S1 in the Supporting Material). All three classes of open state are found within clusters, in which prolonged openings are the predominant ones (relative area 0.57 $\pm$ 0.07). The mean durations remain constant between 0.1 and 3 μM 5-HT. At concentrations

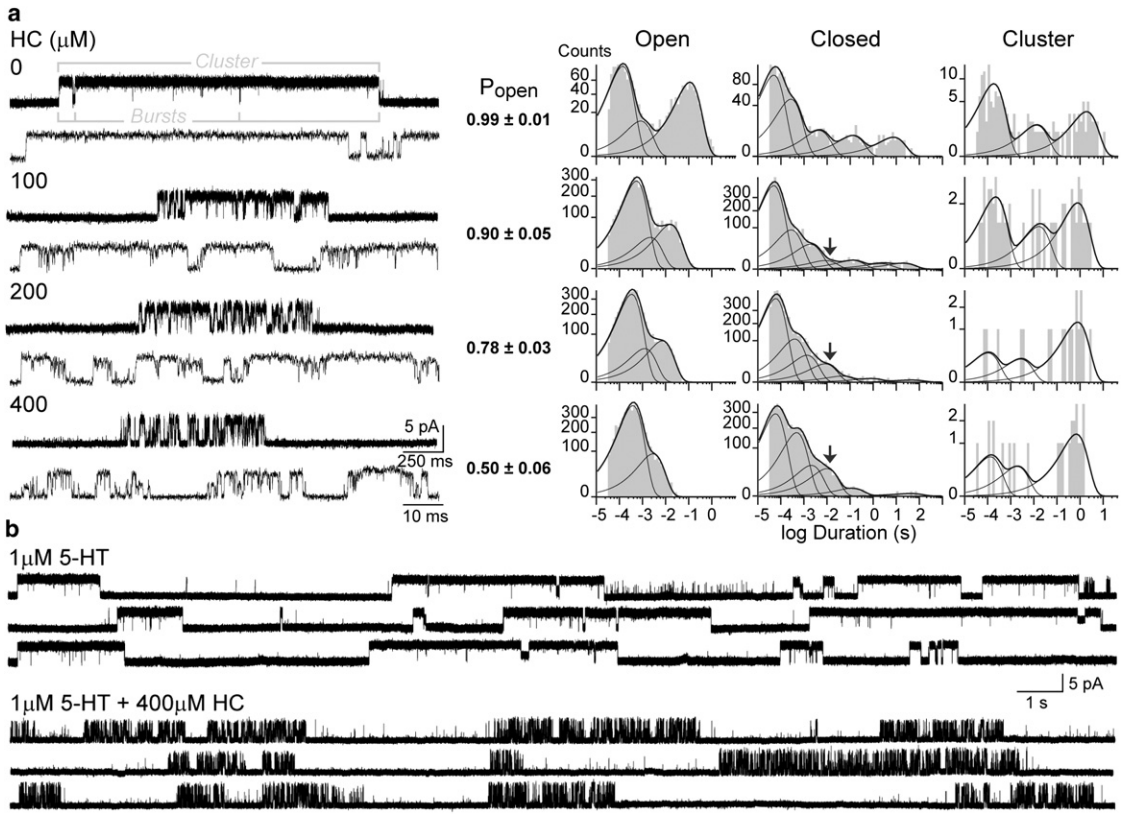

FIGURE 1 Effect of HC on 5-HT$_3$ARs evaluated at the single-channel level. (*a*) *Left*: Channels activated at 1 μM of 5-HT in the absence or presence of increasing HC concentrations in the pipette solution. A single cluster is shown at two different time resolutions for each condition. *Right*: Representative open-, closed-, and cluster-duration histograms obtained from the entire recording at each condition. The arrow shows the 8-ms closed-time component associated with the block. (*b*) Continuous single-channel traces of control and 400-μM-HC-treated channels activated by 1 μM 5-HT. Membrane potential, −70 mV; filter, 10 kHz.

>3 μM, the duration of the slowest open component decreases due to open-channel block produced by 5-HT (18). To avoid blockade, single-channel recordings were performed at 1 μM 5-HT. Closed-time histograms of the entire control recording can be fitted by five to six components (Fig. 1 *a*). Comparison of these histograms with those constructed using only selected clusters show that the two briefest components (~50 μs and ~300 μs) correspond to closings within bursts, and the succeeding one (~2.5 ms) corresponds to interburst closings within clusters (18) (Table S1). The additional slow components observed in histograms constructed with data of the entire recording correspond to closed periods between clusters.

In the presence of HC, significant kinetic changes are observed (Fig. 1). Channel activity at 1 μM 5-HT and 400 μM HC also appears in clusters but these show reduced open probability (P_{open}) (Fig. 1 *b*). This decrease is due to an increase in the duration of dwell times in the closed state and a decrease in the duration of long openings within clusters (Fig. 1). The mean cluster duration shows an approximately twofold reduction at 400 μM HC, from 1.5 ± 0.5 s at 0 μM HC to 0.7 ± 0.2 s at 400 μM HC (Fig. 1 *a* and Table S1). Clusters in the presence of HC are composed of briefer bursts, which in turn are composed of briefer openings. The burst duration is reduced from 850 ± 200 ms (control) to 25 ± 4 ms (400 μM HC), but the number of bursts/cluster is higher than in the control (~30 bursts/cluster for 400 μM HC and ~2–3 bursts/cluster for the control). However, it is not possible to determine whether the bursts in the presence of HC correspond mechanistically to the same bursts as those of the control, which represent transitions through open and closed states (18), or if they arise from a single opening with flickering closings due to open-channel block. The duration of channel openings, particularly that corresponding to the slowest open component, is significantly reduced (~30-fold at 400 μM HC). Closed-time histograms also show several components, but a new closed component with a mean duration of ~8 ms is systematically detected (Fig. 1 *a* and Table S1). Overall, the analysis shows that the cluster is composed of briefer openings separated by brief closings, and by an increased number of bursts that are briefer than the control bursts (Fig. 1).

Open-channel block induced by HC

We analyzed whether the changes in the open, burst, and closed durations can be explained by open-channel block. To this end, we first measured the mean duration of the

slowest open component at different HC concentrations (Fig.1). The mean open duration decreases from 115 ± 20 ms (control) to 11 ± 3 ms, 8 ± 1 ms, and 3.2 ± 0.7 ms at 100, 200, and 400 μM HC, respectively (Table S1). By expressing these results as the inverse of the mean open time versus drug concentration, a linear representation is observed (Fig. S1). This data can be fitted by the classical linear blocking scheme (23) (Scheme 1),

$$C \leftrightarrow O \underset{k_{+b}[HC]}{\leftrightarrow} OB, \qquad \text{(Scheme 1)}$$

where C indicates closed time, O open time (corresponding to the mean duration of the slowest open component), and B the block state. The rate constant for the blocking reaction (k_{+b}), given by the slope of the curve, is 6.5 × 10^5 M^{-1} s^{-1}. Thus, the reduction in open duration may be explained by HC acting as an open-channel blocker.

Given the complexity of the closed-time histograms, it is not possible to clearly distinguish the closed component corresponding to blocked states. One problem is that the duration of the brief intraburst closings observed at 400 μM HC, which may cause the flickering behavior, superimposed with that of brief closings observed in the control, which arise from closings during activation and correspond to the predominant closed component (relative area ~0.6 (Table S1)). In addition, a new closed component is detected (~8 ms), which corresponds to interburst closings and whose area increases with HC concentration. This component could arise from slow channel block (Fig. 1 and Fig. S2).

To gain more insight into the possible mechanism of channel block, we simulated single-channel and macroscopic currents in the presence of 400 μM HC on the basis of the kinetic model that describes activation and desensitization (18) (Fig. S2 *a*). The simulations show that the blocking mechanism is complex and involves at least two blocked states (Fig. S2).

HC favors transitions to the subconductance state

The detailed observation of single-channel recordings from 5-HT$_3$ARs activated by 1 μM 5-HT revealed a minor population of low-amplitude (~2.4 pA) events within clusters (Fig. S3). Subconductance levels occur either isolated or as transitions between full-conductance events. When the analysis is performed by tracking events without any amplitude restriction, the subconductance population is detected in the amplitude histograms as a minor component of ~2.4 pA (Fig. 2 *b*).

In the presence of 400 μM HC, a remarkable increase in the frequency of subconductance levels is observed (Fig. 2 *a*, *lower*). The amplitude histogram clearly reveals

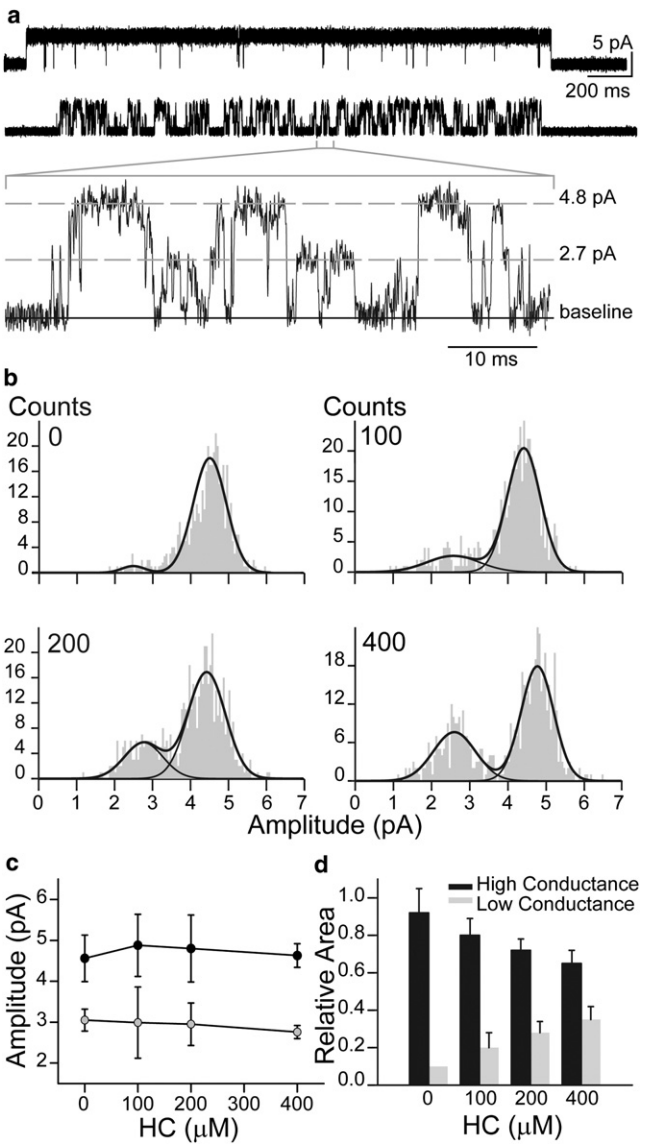

FIGURE 2 HC increases the frequency of the subconductance state. (*a*) A typical cluster of 5-HT$_3$AR activated by 1 μM 5-HT in the absence (*upper*) and presence of 400 μM HC (*lower*), with a segment shown at higher resolution. Membrane potential, −70 mV; filter, 10 kHz. (*b*) Typical amplitude histograms for 0, 100, 200, and 400 μM HC. To determine mean amplitudes, histograms were constructed only with events whose durations were >90 μs. (*c* and *d*) Mean amplitudes (*c*) and relative areas (*d*) resulting from the histograms in *b* for the high- (*black*) and low-conductance events (*gray*) (mean ± SD for at least n = 3 for each condition).

an increase in the relative area of the low-amplitude component of ~2.4 pA, this area being of 0.4 at 400 μM HC.

We examined whether the amplitude of the subconductance events is dependent on HC concentration. To this end, we constructed amplitude histograms from single-channel recordings activated by 1 μM 5-HT in the presence of increasing HC concentrations. Fig. 2 *b* shows that the mean amplitudes of both high- and low-amplitude components remain constant in the range 0–400 μM HC. However, the

relative area of the low-amplitude component increases as a function of HC concentration, whereas that of the high-amplitude component decreases (Fig. 2, *c* and *d*).

The absence of amplitude dependence on drug concentration for the low-conductance events eliminates fast open-channel block as the mechanism mediating the reduction in channel amplitude. Therefore, the results reveal that the 5-HT_3AR opens rarely to a subconductance state and HC increases the probability of adopting this state.

To illustrate changes in the presence of HC, we constructed all-point amplitude histograms. To this end, we analyzed 10–20 clusters from several recordings at each condition. Fig. 3 shows representative histograms for different HC concentrations. In these histograms, 0 corresponds to points in the closed state. The all-point histogram for control clusters shows that most points are concentrated at ~4.7 pA, which corresponds to the main amplitude class. Since these histograms have been constructed only with selected clusters, for which the P_{open} is >0.90, only a minor proportion of points are concentrated at ~0 pA. The increase in resolution shows that there is also a minor population of points at ~2.4 pA, which correspond to subconductance events (Fig. 3, *inset*). The area of this population increases as a function of HC concentration. These histograms also reveal how the P_{open} within clusters decreases as a function of HC. Moreover, because these histograms are constructed only with data from selected clusters, they also demonstrate that subconductance openings occur within a cluster, which in turn reflects the activity of a single receptor channel, and appear in the absence of the drug.

To gain more information about the properties of the subconductance level, we also evaluated how its amplitude and relative area change as a function of membrane potential and HC concentration. The amplitudes of both full conductance (~4.7 pA) and subconductance openings (~2.4 pA) remain constant for 0–400 μM HC at a fixed membrane potential, and they similarly increase when the membrane potential decreases from −70 to −120 mV (Fig. 4, *a* and *b*). Fig. 4, *c* and *d*, shows that the relative area of the low-conductance events tends to increase at −120 mV with respect to −70 mV. The difference is statistically significant only at 400 μM HC and between −70 mV and −120 mV ($p < 0.05$). At 400 μM HC and negative membrane potentials, the relative area of subconductance events increases e-fold/165 mV, whereas in the absence of HC, it increases e-fold/550 mV. Thus, the increase in the frequency of subconductance events due to HC seems to be slightly dependent on potential.

Because the analysis of single channels at positive membrane potentials is very complex and less accurate, these experiments could be performed only for a restricted negative membrane potential range.

To determine the duration of the subconductance state, we analyzed recordings at a fixed amplitude of 2.4 pA. In the absence of HC, open-time histograms can be fitted by two components, whose duration and relative areas are 500 ± 10 μs (0.20 ± 0.07) and 2.3 ± 0.2 ms (n = 3). In the presence of 400 μM HC, the duration of the open components is reduced to 80 ± 10 μs and 240 ± 70 μs (n = 3). It is important to note that the measured durations are prolonged enough to be fully resolved (see Methods), giving

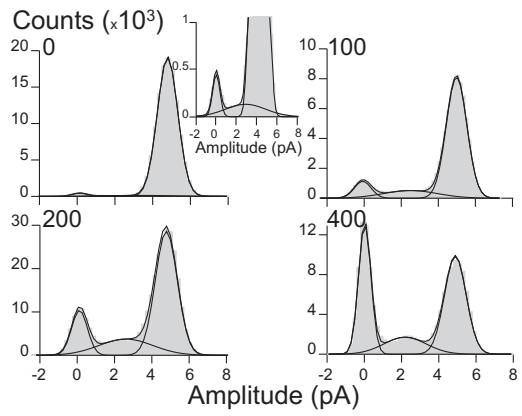

FIGURE 3 All-point amplitude histograms from clusters in the presence of HC concentrations of 0, 100, 200, and 400 μM. About 20 clusters from three different recordings for each condition were selected and analyzed. In these histograms, points at 0 pA correspond to points in the closed state. Points corresponding to low-amplitude events (~2.4 pA) appear in some recordings even in the absence of HC, though at a very low frequency. (*Inset*) A higher-resolution histogram showing the appearance of these low amplitude events even in the control. The relative areas for the 0- and 2.4-pA components increase as a function of HC concentration.

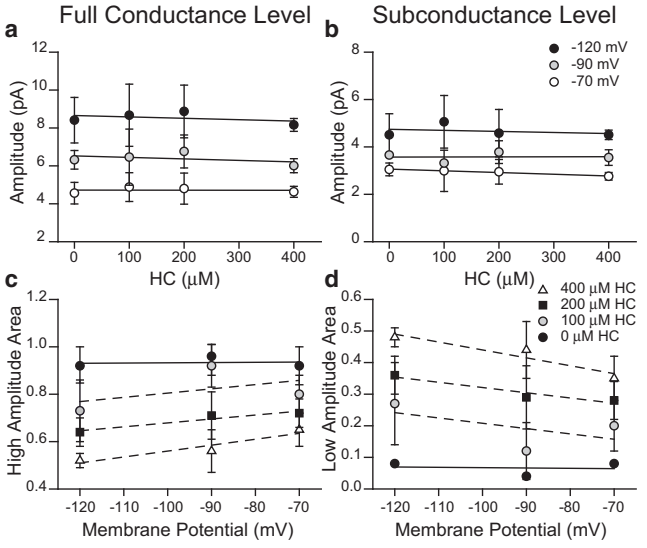

FIGURE 4 Amplitude and relative area of the full (*a* and *c*) and subconductance levels (*b* and *d*) as a function of HC concentration and membrane potential. (*a* and *b*) Mean amplitude of the full (*a*) and subconductance levels (*b*) at −120, −90, and −70 mV as a function of HC concentration. (*c* and *d*) Relative areas of the full (*c*) and subconductance levels (*d*) at different HC concentrations as a function of membrane potential. Values are presented as mean ± SD for at least three patches for each condition.

confidence that these current levels are a result of a different channel conformation and not an artifact produced by limited bandwidth (Fig. S3).

Dual effect of HC on 5-HT$_3$A macroscopic currents

To study the overall consequences of HC on 5-HT$_3$A activation, we recorded macroscopic currents from outside-out patches perfused with 100 μM 5-HT in the absence and presence of 400 μM HC. 5-HT-activated currents decay during the pulse of agonist with a double exponential function (18,24). We verified that the currents remained stable for several 5-HT pulses, indicating the absence of rundown (Fig. 5 *a*).

To determine the conformational state at which the drug acts, we recorded currents applying 5-HT and HC under different protocols (pipette potential −50 mV). To determine whether the drug affects the resting state, we first activated receptors by 100 μM 5-HT in the absence of HC as a control pulse (−/− protocol). Then we exposed the patch for 2 min to ECS containing 400 μM HC and finally elicited currents with ECS containing 5-HT (+/− protocol) (test pulse). Comparison of currents obtained from the test pulse to those obtained from the control pulse shows an ~40% reduction in the peak current (Fig. 5, *b* and *e*). No statistically significant changes in the decay time constants are observed (t_{fast} of 170 ± 50 ms and t_{slow} of 1100 ± 650 ms for the −/− protocol (n = 4); and t_{fast} of 110 ± 40 ms and t_{slow} of 650 ± 400 ms for the +/− protocol (n = 4) (Fig. 5, *b* and *f*)). Activation of receptors in the presence of HC (ECS containing 400 μM HC + 100 μM 5-HT) without preincubation with the steroid (−/+ protocol) reduces current amplitude by ~45% with respect to the control (Fig. 5, *c* and *e*). It is interesting to note that under this protocol, the decay time constants decrease significantly (t_{fast} of 20 ± 10 ms and t_{slow} of 270 ± 100 ms (n = 4)) (Fig. 5 *f*). The currents decrease to a similar extent if 5-HT concentration is 3, 100, or 500 μM, thus discarding the possibility that HC acts as a competitive antagonist (Fig. S5). Moreover, similar changes occur in the low-conductance wild-type 5-HT$_3$A receptor, thus indicating that the mutations that alter conductance do not affect significantly HC action (Fig. S5).

After a 5-min wash with ECS, the original peak current could not be recovered in 70% of the patches under the +/− protocol and in 100% under the −/+ protocol. It was verified that the HC-mediated decrease in peak currents was not due to rundown (Fig. S6). In contrast, recovery of control decay time constants always occurred after a 2-min wash.

When the patch is continuously exposed to HC (+/+ protocol), currents show the greatest amplitude inhibition (~50%) and the control peak currents are not recovered after a 5-min wash (Fig. 5, *d* and *e*). The percentage of reduction obtained with this protocol is not completely

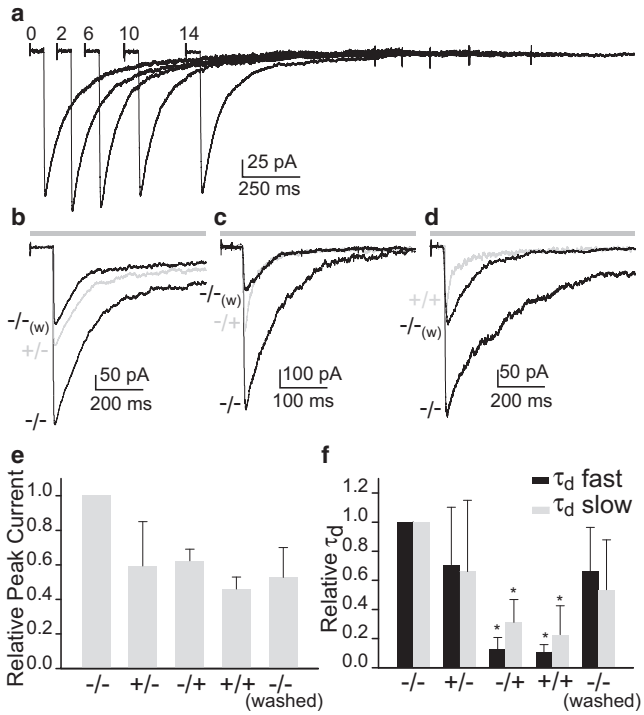

FIGURE 5 Effect of HC on macroscopic 5-HT$_3$A currents. (*a*) Representative 100 μM 5-HT response (filter, 5 kHz) recorded from a single outside-out patch, showing that the current remains stable for 14 min. (*b*) Exposure to HC (2 min) before application of 5-HT (+/− protocol, *gray trace*). (*c*) Simultaneous application of HC and 5-HT without preincubation with the drug (−/+ protocol, *gray trace*). (*d*) Preexposure with HC followed by application of HC and 5-HT (+/+ protocol). For all protocols (*b–d*), currents were compared with those recorded from the same patch before any drug application (−/− protocol, *black traces*). Also, currents recorded after washing the drug are shown for all protocols (−/−$_{(w)}$, *black traces*). For each experiment, the peak current (*e*) and the decay time constants of both components (t_{fast} and t_{slow}) (*f*) were related to those of the control. The description washed corresponds to currents recorded after a 5-min wash of the drug in the +/+ protocol. The bars correspond to the mean ± SD of at least three different experiments for each condition. Pipette potential, −50 mV. The bars above the currents in *b*, *c*, and *d* correspond to the application of 100 μM 5-HT. Please note that because of space limitation, the whole pulse (1.5 s) is not represented by the bar.

additive with respect to that observed when the drug acts only at the closed (+/− protocol) or open (−/+ protocol) states (Fig. 5 *e*). Similar to what is observed under the −/+ protocol, the decay time constants decrease with respect to control (t_{fast} of 16 ± 6 ms and t_{slow} of 180 ± 60 ms (n = 4)) and are rapidly recovered after the wash (Fig. 5 *f*).

We conclude that once the receptors have been exposed to HC, the reduction in the peak current is slowly reversible. More precisely, it is irreversible for at least 5 min, which is the maximal time that systematically ensures stability of outside-out patches for the entire experiment. In contrast, the decrease in the decay time constants is rapidly reversible after the wash. Also, whereas the decrease in peak current occurs independently of the state at which HC acts (closed

or open), the HC-mediated increase in the decay rates occurs mainly from the open state (−/+ protocol).

Taken together, our results reveal that HC exerts its inhibitory action by at least two different mechanisms. One mechanism is channel block, which is evidenced at the single-channel level mainly as a dramatic decrease in open duration, burst duration, and P_{open} within clusters. The other mechanism is an increase in the frequency at which the receptor opens to a subconductance state. The combination of both effects is evidenced at the macroscopic level by a reduction in current amplitude, which occurs when HC acts from either open or closed states, and an increase in the decay rates, which occurs when HC acts from the open state.

DISCUSSION

Single-channel recordings have allowed the description of mechanisms of action of steroids at AChRs (6,25,26) and $GABA_A$ receptors (12,27). In contrast, for 5-HT_3ARs, the effects of steroids have been studied only at the macroscopic current level because of its low conductance. However, the high-conductance form is a valid model for understanding activation and modulation mechanisms of wild-type receptors, since the triple mutation does not affect profoundly the activation parameters (18,28). In human 5-HT_3AR, the EC_{50} has been shown to change slightly from 3 μM to 1.1 μM due to the QDA mutation (16). Moreover, deletion of the entire M3-M4 loop mainly affects channel conductance (29). However, as it is not possible to discard the possibility that the triple mutation introduces slight kinetic changes that can be detected mainly at the single-channel level, the high-conductance receptor should be considered a model. Nevertheless, we here show that the overall changes produced by HC are similar for wild-type and high-conductance 5-HT_3ARs.

The concentration of HC attainable in blood after a single intravenous 100-mg dose is ~3 μM (30). HC may be administrated more frequently, and it may be accumulated in biological membranes, which may significantly increase its effective concentration and may therefore affect 5-HT_3A function. Significant inhibition of the 5-HT_3AR function by different steroids has been observed at concentrations varying between 2 μM and 1 mM (8–10). Given that the potency may govern the physiological relevance of steroid inhibition, it would be interesting to determine, at the single-channel level, whether such a wide spectrum is due to different mechanisms of action.

Striking features of single-channel activity of QDA 5-HT_3ARs is that openings appear grouped in bursts, which in turn coalesce into long clusters of ~1.5 s. The P_{open} and mean duration of intracluster closings do not depend on agonist concentration (18). We here show that HC produces dramatic changes in this pattern activity. Activity appears in clusters of reduced P_{open} and composed of increased numbers of briefer bursts and openings.

A noticeable effect of HC is the dose-dependent reduction in the duration of openings (~30-fold at 400 μM HC). The relationship between the inverse of the duration of the slowest open component, which is the main one within clusters in control recordings, and HC concentration is compatible with the steroid acting as an open-channel blocker (23). On the basis of Scheme 1, if HC dissociates quite rapidly, openings would be expected to occur in bursts as the channel blocks and unblocks several times before entering a closed period. Therefore, it is possible that the bursts observed in the presence of HC correspond to a single opening event interrupted by flickering closings due to rapid blocking and unblocking. Given the complexity of the closed time histograms, it is not possible to identify closings corresponding to these blocked periods as their duration overlap with that of brief closings that separate openings within bursts in the absence of the drug and that result from receptor activation process and not from blocking (18). However, on the basis of the typical open-channel block (Scheme 1), the burst duration should increase with blocker concentration (31), in contrast to our observations. Moreover, simulation of single channels on the basis of a linear open-channel block model does not well describe the experimental data, revealing that the blocking mechanism deviates from that of classical open-channel blockers. Deviations from the linear open-channel block mechanism have been described for many noncompetitive antagonists, including HC in AChRs (5,6,25,31). They can take place, for example, if open-channel block is combined with closing of the blocked receptor (31–33), or if there are two or more blocking sites in the pore (34,35). Our simulation studies show that models with two blocked states, open or closed, can explain more closely the observed changes in cluster properties, but the relative areas of the open components of the simulated data differ from the corresponding experimental data. One explanation could be that subconductance levels within clusters were not considered during simulation. Also, it could be possible that HC produces direct changes in activation kinetics, in addition to acting as an open channel blocker.

The increase in the fast decay rate may reflect fast open-channel block, which is clearly detected at the single-channel level by the decrease in mean open time, and the increase in the slow decay rate may correspond to slow block. It also could be possible that the slight decrease in the cluster duration and in the slow decay rate is mediated by a slight increase in the desensitization rate. Unfortunately, distinguishing between channel block with a slow unblocking rate and increased desensitization is not possible from this type of experiment (36,37). Nevertheless, the high channel activity observed in the presence of HC suggests that the drug does not produce significant stabilization of desensitized states.

Interestingly our experiments reveal that in addition to its action as a complex open-channel blocker, HC acts by what we believe to be a novel mechanism: it increases the frequency of the subconductance state. In 5-HT$_3$ARs, as well as in other Cys-loop receptors, a very infrequent population of low-conductance openings is detected (18). Since these events occur within clusters, which correspond to activation periods of the same receptor molecule, we can infer that they reflect a subconductance state of the same receptor. The apparent mean open time of the subconductance state is briefer than that of the full amplitude state at the same HC concentration, although it is long enough to be well resolved. Thus, the stability at this open conformation is lower than the normal open conformation.

Although fast blockers can induce closures so brief that single-channel amplitude appears to be attenuated (35), we can discard fast open-channel block as the explanation for the increased frequency of subconductance events, because a concentration-dependent decrease of channel amplitude should have been observed instead. Also, the amplitude of the subconductance level is similar in the absence and presence of HC, thus suggesting that the drug only increases the frequency at which the channel adopts the subconductance level. An alternative explanation is that HC produces a stable and partial sterical occlusion of the pore by acting at the vestibule in the conduction pathway (38).

During a pulse of 100 μM 5-HT, current decays are fitted by two components (18,28). When outside-out patches are continuously exposed to HC, the amplitude of currents is reduced and currents decay more rapidly. The application of HC under different protocols provided information about the conformational state at which HC is acting. The reduction in the peak current occurs for all protocols, i.e., if HC is applied before (+/−) or during (−/+) channel opening. Under fast perfusion, the peak current is the result of the number of channels in the patch, the probability of channel opening, and the single-channel amplitude. Therefore, such reduction may originate from both the decrease in the P_{open} and the increase in the frequency of opening to the subconductance level. This reduction is independent of the conformational state (closed or open), and it cannot be recovered rapidly after washing the drug, indicating that dissociation of the drug from this site is slow. The current decay rate for macroscopic currents increases only when HC is applied together with 5-HT (−/+ protocol), thus supporting open-channel block. This effect, in contrast to the reduction of the peak current, is rapidly reversible. Although it is not possible to determine whether subconductance events also occur in wild-type 5-HT$_3$ARs, the similar decrease in the peak current observed between QDA and wild-type receptors suggests that HC acts similarly in both receptors.

Thus, results at both the single-channel and macroscopic current level indicate that HC acts by at least two different mechanisms, and probably at different sites. 5-HT$_3$ARs may have a site for HC at the pore, from where the drug mediates open-channel block that is rapidly reversed after the wash and is evidenced by the reduction of channel lifetime. HC may also act at a second site, from where it increases the frequency of the subconductance state. This site can be reached if the channel is open or closed, indicating that it may be located in the vestibule of the ion conduction pathway (from where it may produce partial occlusion) or outside the pore. The slight dependency on membrane potential suggests that it may be within the membrane region. We cannot discard the possibility that HC occupies only one site, from which it produces two different effects. However, under this hypothesis, it is difficult to explain the distinct reversibility behavior of both effects. The sites of action of steroids on Cys-loop receptors have not been elucidated. Several lines of experimental evidence in both AChRs (6,39) and GABA$_A$ receptors (7,40) suggest that steroids may interact with membrane-exposed regions of the receptors and that partitioning into the plasma membrane is an important step for effective modulation. To verify whether HC might occupy a region outside the ion pore, we docked HC into a homology model containing two adjacent 5-HT3A subunits (Fig. 6). The most favorable positions (77%) were found within the transmembrane domain, at the extracellular third level of the helices

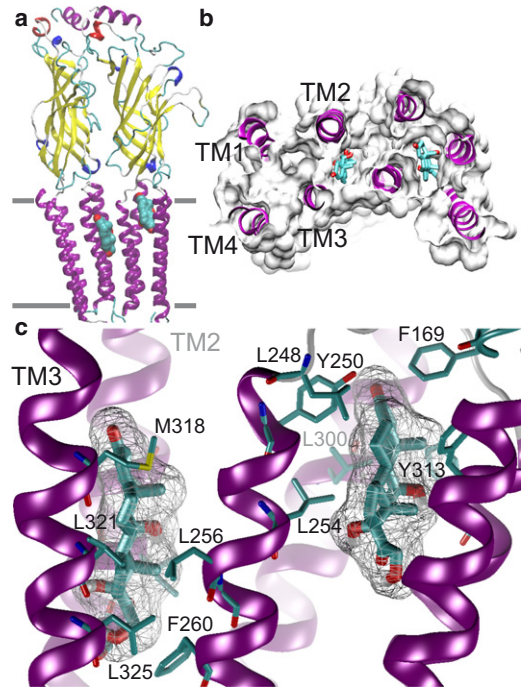

FIGURE 6 Computer docking of HC in 5-HT$_3$A. (*a*) Model of two adjacent 5-HT3A subunits based on *Torpedo* AChR (Protein Data Bank code 2BG9) with HC docked. (*b*) Transmembrane region viewed from the synaptic cleft, showing HC docked into inter- and intrasubunit sites (*left* and *right sites*, respectively). These positions were found in 77% of the docking runs. (*c*) Close-up view of HC docked into inter- and intrasubunit sites (*left* and *right sites*, respectively).

(Fig. 6 *a*). Docking revealed two different sites that could be reached through a membrane pathway. In one site (38% of the docking runs), HC is located at the interface between adjacent subunits, and in the other site (39%), it is located at a hydrophobic cavity between the transmembrane helices of a subunit (Fig. 6 *b*). In both cases, HC interacts with hydrophobic residues and is stabilized by hydrogen bonds (Fig. 6 *c*). It is interesting to note that the intrasubunit site is close to a phenylalanine of the Cys-loop, whose crucial role in channel gating has been demonstrated for all family members (41). The pore of Cys-loop receptors is lined by the M2 domains of the five subunits (42,43). Although various authors have proposed different molecular rearrangements underlying channel opening, the fundamental motion of M2 that opens the pore remains unknown (41–46). Until the mechanisms of channel opening and conduction are deciphered, we can only speculate about the origin of the subconductance level. It could be that subconductance levels arise from movements of fewer than five M2 segments. This interpretation could be similar to that derived from single-channel analysis of drk1 K channels (47). An alternative mechanism is that subconductance levels may be produced by quantitative or qualitative changes in the normal M2 movements elicited after agonist binding. Thus, HC may bind to the intrasubunit, the intersubunit, or to both sites, leading to a distortion of the M2 movements during gating.

In addition to describing what we believe to be a novel mechanism of steroid modulation of 5-HT_3ARs, this study opens the door to examining the intriguing origin of subconductance levels, which have been shown to occur in all members of the Cys-loop receptor family (48,49).

SUPPORTING MATERIAL

Six figures and one table are available at http://www.biophysj.org/biophysj/supplemental/S0006-3495(10)01364-0.

This work was supported by grants from Universidad Nacional del Sur, Agencia Nacional de Promoción Científica y Tecnológica, and Consejo Nacional de Investigaciones Científicas y Técnicas (C.B.).

REFERENCES

1. Barnes, N. M., T. G. Hales, …, J. A. Peters. 2009. The 5-HT3 receptor—the relationship between structure and function. *Neuropharmacology.* 56:273–284.
2. Faerber, L., S. Drechsler, …, W. Fischer. 2007. The neuronal 5-HT3 receptor network after 20 years of research—evolving concepts in management of pain and inflammation. *Eur. J. Pharmacol.* 560:1–8.
3. Thompson, A. J., and S. C. Lummis. 2007. The 5-HT3 receptor as a therapeutic target. *Expert Opin. Ther. Targets.* 11:527–540.
4. Akk, G., D. F. Covey, …, S. Mennerick. 2007. Mechanisms of neurosteroid interactions with GABA(A) receptors. *Pharmacol. Ther.* 116:35–57.
5. Arias, H. R., P. Bhumireddy, and C. Bouzat. 2006. Molecular mechanisms and binding site locations for noncompetitive antagonists of nicotinic acetylcholine receptors. *Int. J. Biochem. Cell Biol.* 38:1254–1276.
6. Bouzat, C., and F. J. Barrantes. 1996. Modulation of muscle nicotinic acetylcholine receptors by the glucocorticoid hydrocortisone. Possible allosteric mechanism of channel blockade. *J. Biol. Chem.* 271:25835–25841.
7. Chisari, M., L. N. Eisenman, …, C. F. Zorumski. 2010. The sticky issue of neurosteroids and $GABA_A$ receptors. *Trends Neurosci.* 33: 299–306.
8. Suzuki, T., M. Sugimoto, …, I. Uchida. 2004. Inhibitory effect of glucocorticoids on human-cloned 5-hydroxytryptamine3A receptor expressed in *Xenopus* oocytes. *Anesthesiology.* 101:660–665.
9. Wetzel, C. H., B. Hermann, …, R. Rupprecht. 1998. Functional antagonism of gonadal steroids at the 5-hydroxytryptamine type 3 receptor. *Mol. Endocrinol.* 12:1441–1451.
10. Oz, M., L. Zhang, and C. E. Spivak. 2002. Direct noncompetitive inhibition of 5-HT_3 receptor-mediated responses by forskolin and steroids. *Arch. Biochem. Biophys.* 404:293–301.
11. Curtis, L., B. Buisson, …, D. Bertrand. 2002. Potentiation of human $\alpha4\beta2$ neuronal nicotinic acetylcholine receptor by estradiol. *Mol. Pharmacol.* 61:127–135.
12. Li, P., A. K. Bandyopadhyaya, …, G. Akk. 2009. Hydrogen bonding between the 17β-substituent of a neurosteroid and the $GABA_A$ receptor is not obligatory for channel potentiation. *Br. J. Pharmacol.* 158:1322–1329.
13. Kelley, S. P., J. I. Dunlop, …, J. A. Peters. 2003. A cytoplasmic region determines single-channel conductance in 5-HT_3 receptors. *Nature.* 424:321–324.
14. Hales, T. G., J. I. Dunlop, …, J. A. Peters. 2006. Common determinants of single channel conductance within the large cytoplasmic loop of 5-hydroxytryptamine type 3 and $\alpha4\beta2$ nicotinic acetylcholine receptors. *J. Biol. Chem.* 281:8062–8071.
15. Deeb, T. Z., J. E. Carland, …, T. G. Hales. 2007. Dynamic modification of a mutant cytoplasmic cysteine residue modulates the conductance of the human 5-HT_3A receptor. *J. Biol. Chem.* 282:6172–6182.
16. Livesey, M. R., M. A. Cooper, …, J. A. Peters. 2008. Structural determinants of Ca^{2+} permeability and conduction in the human 5-hydroxytryptamine type 3A receptor. *J. Biol. Chem.* 283:19301–19313.
17. Peters, J. A., T. G. Hales, and J. J. Lambert. 2005. Molecular determinants of single-channel conductance and ion selectivity in the Cys-loop family: insights from the 5-HT_3 receptor. *Trends Pharmacol. Sci.* 26:587–594.
18. Corradi, J., F. Gumilar, and C. Bouzat. 2009. Single-channel kinetic analysis for activation and desensitization of homomeric 5-HT_3A receptors. *Biophys. J.* 97:1335–1345.
19. Bouzat, C., M. Bartos, …, S. M. Sine. 2008. The interface between extracellular and transmembrane domains of homomeric Cys-loop receptors governs open-channel lifetime and rate of desensitization. *J. Neurosci.* 28:7808–7819.
20. Rayes, D., M. J. De Rosa, …, C. Bouzat. 2009. Number and locations of agonist binding sites required to activate homomeric Cys-loop receptors. *J. Neurosci.* 29:6022–6032.
21. Sali, A., and T. L. Blundell. 1993. Comparative protein modelling by satisfaction of spatial restraints. *J. Mol. Biol.* 234:779–815.
22. Goodsell, D. S., G. M. Morris, and A. J. Olson. 1996. Automated docking of flexible ligands: applications of AutoDock. *J. Mol. Recognit.* 9:1–5.
23. Neher, E., and J. H. Steinbach. 1978. Local anaesthetics transiently block currents through single acetylcholine-receptor channels. *J. Physiol.* 277:153–176.
24. Mott, D. D., K. Erreger, …, S. F. Traynelis. 2001. Open probability of homomeric murine 5-HT_3A serotonin receptors depends on subunit occupancy. *J. Physiol.* 535:427–443.
25. Bouzat, C., and F. J. Barrantes. 1993. Hydrocortisone and 11-desoxycortisone modify acetylcholine receptor channel gating. *Neuroreport.* 4:143–146.

26. Paradiso, K., K. Sabey, …, J. H. Steinbach. 2000. Steroid inhibition of rat neuronal nicotinic $\alpha4\beta2$ receptors expressed in HEK 293 cells. *Mol. Pharmacol.* 58:341–351.
27. Akk, G., D. F. Covey, …, S. Mennerick. 2009. The influence of the membrane on neurosteroid actions at $GABA_A$ receptors. *Psychoneuroendocrinology.* 34 (*Suppl 1*):S59–S66.
28. Solt, K., D. Ruesch, …, D. E. Raines. 2007. Differential effects of serotonin and dopamine on human 5-HT_3A receptor kinetics: interpretation within an allosteric kinetic model. *J. Neurosci.* 27:13151–13160.
29. Jansen, M., M. Bali, and M. H. Akabas. 2008. Modular design of Cys-loop ligand-gated ion channels: functional 5-HT_3 and GABA rho1 receptors lacking the large cytoplasmic M3M4 loop. *J. Gen. Physiol.* 131:137–146.
30. Petitjean, O., J. L. Wendling, …, A. Astier. 1992. Pharmacokinetics and absolute rectal bioavailability of hydrocortisone acetate in distal colitis. *Aliment. Pharmacol. Ther.* 6:351–357.
31. Dilger, J. P., R. S. Brett, and L. A. Lesko. 1992. Effects of isoflurane on acetylcholine receptor channels. 1. Single-channel currents. *Mol. Pharmacol.* 41:127–133.
32. Amador, M., and J. A. Dani. 1991. MK-801 inhibition of nicotinic acetylcholine receptor channels. *Synapse.* 7:207–215.
33. Neher, E. 1983. The charge carried by single-channel currents of rat cultured muscle cells in the presence of local anaesthetics. *J. Physiol.* 339:663–678.
34. Akk, G., and J. H. Steinbach. 2000. Activation and block of recombinant $GABA_A$ receptors by pentobarbitone: a single-channel study. *Br. J. Pharmacol.* 130:249–258.
35. Dilger, J. P., R. Boguslavsky, …, A. M. Vidal. 1997. Mechanisms of barbiturate inhibition of acetylcholine receptor channels. *J. Gen. Physiol.* 109:401–414.
36. Papke, R. L., and R. E. Oswald. 1989. Mechanisms of noncompetitive inhibition of acetylcholine-induced single-channel currents. *J. Gen. Physiol.* 93:785–811.
37. Gumilar, F., H. R. Arias, …, C. Bouzat. 2003. Molecular mechanisms of inhibition of nicotinic acetylcholine receptors by tricyclic antidepressants. *Neuropharmacology.* 45:964–976.
38. Tsushima, R. G., J. E. Kelly, and J. A. Wasserstrom. 2002. Subconductance activity induced by quinidine and quinidinium in purified cardiac sarcoplasmic reticulum calcium release channels. *J. Pharmacol. Exp. Ther.* 301:729–737.
39. Santiago, J., G. R. Guzmàn, …, J. A. Lasalde-Dominicci. 2001. Probing the effects of membrane cholesterol in the *Torpedo californica* acetylcholine receptor and the novel lipid-exposed mutation α C418W in *Xenopus* oocytes. *J. Biol. Chem.* 276:46523–46532.
40. Hosie, A. M., M. E. Wilkins, …, T. G. Smart. 2006. Endogenous neurosteroids regulate $GABA_A$ receptors through two discrete transmembrane sites. *Nature.* 444:486–489.
41. Bartos, M., J. Corradi, and C. Bouzat. 2009. Structural basis of activation of cys-loop receptors: the extracellular-transmembrane interface as a coupling region. *Mol. Neurobiol.* 40:236–252.
42. Miyazawa, A., Y. Fujiyoshi, and N. Unwin. 2003. Structure and gating mechanism of the acetylcholine receptor pore. *Nature.* 423:949–955.
43. Unwin, N. 2005. Refined structure of the nicotinic acetylcholine receptor at 4 Å resolution. *J. Mol. Biol.* 346:967–989.
44. Cymes, G. D., Y. Ni, and C. Grosman. 2005. Probing ion-channel pores one proton at a time. *Nature.* 438:975–980.
45. Hilf, R. J., and R. Dutzler. 2009. Structure of a potentially open state of a proton-activated pentameric ligand-gated ion channel. *Nature.* 457:115–118.
46. Taly, A., M. Delarue, …, J. P. Changeux. 2005. Normal mode analysis suggests a quaternary twist model for the nicotinic receptor gating mechanism. *Biophys. J.* 88:3954–3965.
47. Chapman, M. L., and A. M. VanDongen. 2005. K channel subconductance levels result from heteromeric pore conformations. *J. Gen. Physiol.* 126:87–103.
48. Dani, J. A., and J. A. Fox. 1991. Examination of subconductance levels arising from a single ion channel. *J. Theor. Biol.* 153:401–423.
49. Hamill, O. P., J. Bormann, and B. Sakmann. 1983. Activation of multiple-conductance state chloride channels in spinal neurones by glycine and GABA. *Nature.* 305:805–808.